Spatial Patterns of Glaciers in Response to Spatial Patterns in Regional Climate

KATHLEEN HUYBERS AND GERARD H. ROE

Department of Earth and Space Sciences, University of Washington, Seattle, Washington

ABSTRACT

Glaciers are direct recorders of climate history and have come to be regarded as emblematic of climate change. They respond to variations in both accumulation and ablation, which can have separate atmospheric controls, leading to some ambiguity in interpreting the causes of glacier changes. Both climate change and climate variability have characteristic spatial patterns and time scales. The focus of this study is the regional-scale response of glaciers to natural patterns of climate variability. Using the Pacific Northwest of North America as the setting, the authors employ a simple linear glacier model to study how the combination of patterns of melt-season temperature and patterns of annual accumulation produce patterns of glacier length variations. Regional-scale spatial correlations in glacier length variations reflect three factors: the spatial correlations in precipitation and melt-season temperature, the geometry of a glacier and how it determines the relative importance of temperature and precipitation, and the climatic setting of the glaciers (i.e., maritime or continental). With the self-consistent framework developed here, the authors are able to evaluate the relative importance of these three factors. The results also highlight that, in order to understand the natural variability of glaciers, it is critically important to know the small-scale patterns of climate in mountainous terrain. The method can be applied to any area containing mountain glaciers and provides a baseline expectation for natural glacier variation against which the effects of climate changes can be evaluated.

1. Introduction

A major goal in current climate research lies in understanding patterns in climate and how they translate to climate proxies. Glaciers are among the most closely studied of these proxies because they respond directly to both snow accumulation and surface energy balance. These, in turn, reflect the precipitation and melt-season temperature of the regional climate (Ohmura et al. 1992). A glacier's response to this climate is most often characterized by a change in the position of its terminus. Records of terminus advance and retreat are readily available in both the geologic and historic record through the formation of moraines, lichenometry, aerial photography, cosmogenic dating, and satellite imagery. Beyond the period of the instrumental record, well-dated glacial deposits often serve as the primary descriptor of the climate history of a region.

Despite the direct nature of a glacier's response to climate, the current near-global retreat as well as past glacier variations both present complicated pictures. Though there is strong evidence that glaciers worldwide are presently retreating (e.g., Oerlemans 2005), individual glaciers vary in the magnitude of response. In a few locations, glaciers have even advanced during the past decades, as is the case in Norway and New Zealand (e.g., Nesje 2005; Chinn et al. 2005). Moreover, some well-documented retreats like that on Mount Kilimanjaro have complicated causes that are not easily explained (e.g., Mölg and Hardy 2004). While there is often local coherence among glacial advances and retreats, it has proven harder to extrapolate these results across continental-scale regions (e.g., Rupper and Roe 2008).

The difficulty in interpreting terminus advance and retreat is threefold. First, glaciers are not indicators of a single atmospheric variable. They reflect the effect of many atmospheric fields, primarily accumulation and temperature, but also cloudiness, wind, longwave and shortwave radiation balances, the turbulent fluxes of sensible and latent heat, and humidity, among others. Second, each glacier is subject to a particular combination of the bed slope, hypsometry, accumulation area,

Corresponding author address: Kathleen Huybers, Department of Earth and Space Sciences, University of Washington, Box 351310, Seattle, WA 98195.
E-mail: khuybers@u.washington.edu

debris cover, local shading, etc., creating a setting that is unique to each glacier. Finally, glaciers integrate the interannual variability of the climate over many years or even decades; the advance or retreat of a glacier cannot be traced to a single year's climate.

Hence, in order to understand how spatial patterns in climate variability translate into spatial patterns of glacial response, we must systematically analyze patterns in regional climate and model a glacier's response to the dominant variables. These patterns of climate variability and glacier response must be understood in order to establish the natural variability of a glacier (i.e., the variability in the absence of an external climate forcing). It is only when observed responses exceed this expected natural variability that glaciers can be said to be recording a true regional, hemispheric, or global climate change (e.g., Reichert et al. 2002; Roe and O'Neal 2009, hereafter RO).

The goal of this paper is to derive and analyze a model of the expected regional-scale correlations of glacier length variations in response to interannual variability in precipitation and melt-season temperature. We take a first-order approach to this problem, using the simplest model framework capable of representing how glaciers amalgamate different aspects of climate to produce terminus variations. In particular, we address the following questions:

1) What are the spatial patterns of variability in precipitation and melt-season temperature?
2) How do these patterns of intrinsic climate variability translate into patterns of glacier advance and retreat?
3) Over what spatial extent can we expect these intrinsic, natural fluctuations of glaciers to be correlated?

We use a simple linear glacier model that has been shown to adequately capture recent glacier variability (Jóhannesson et al. 1989; Oerlemans 2005; RO). The patterns we find in our results are consistent with those of other glacier mass balance studies (Harper 1993; Bitz and Battisti 1999). The advantage of our approach is that it allows us to explore such patterns on a wider, regional scale and to understand in detail the relative importance of the different causes.

Our modeled patterns of glacier advance and retreat are not intended to simulate either the recent or the paleorecord of glacier advance and retreat. First, this is because we have chosen to explore only the interannual variability of climate and have removed any trend from the data. Second, and more fundamentally, accounting for the processes that build up and deposit moraines on the landscape, and particularly the time scale of their formation, is beyond the scope of our chosen model

(e.g., Putkonen and O'Neal 2006). We regard our results, therefore, as a means to explore how climate patterns are combined through the dynamical glacier system and as an aid in the interpretation of glacial landscape features.

2. Setting and data

Our study area is the Pacific Northwest, covering the northwestern United States, British Columbia, and southern Alaska. This region is ideal because of the large number of well-documented glaciers, the different climatic environments, and the range of glacier sizes that exist in the region. The dominant climate patterns in the area are also well understood. Figure 1 maps the locations of all major glaciers in the region.

Our principal climate dataset is that of Legates and Willmott (1990a,b), hereafter denoted LW50, which provides 50 years of worldwide temperature and precipitation station data interpolated onto a $0.5° \times 0.5°$ grid. We extract from this dataset two atmospheric variables that reflect the most important climatic forcing for glaciers. The first variable is the melt-season temperature, which we define as the average surface temperature between June and September (JJAS). For simplicity, we assume that the ablation rate is directly proportional to the melt-season temperature, as suggested by observations (e.g., Paterson 1994; Ohmura et al. 1996). The second variable is the mean annual precipitation, which, again for simplicity, we assume reflects the accumulation of snowfall on a putative glacier within any grid point. Approximately 80% of precipitation in this region comes in the fall and wintertime (e.g., Hamlet et al. 2005). To distinguish in more detail between precipitation and snowfall would require extrapolation onto high-resolution topographic digital elevations models. The data are linearly detrended in order to identify the internal variability in these climate variables and, so, neglect any recent warming.

These simplifications are appropriate for the first-order approach in this study, its focus on the regional-scale response, and the relatively coarse 0.5°-resolution data that does not reflect detailed small-scale orographic features. We discuss refinements of the model framework in section 5 and the discussion.

a. Climate in the Pacific Northwest

Figures 2a and 2b depict the mean annual precipitation and the mean melt-season temperature over the region. The Cascade, Olympic, Coast, and St. Elias Mountains are important influences on the region's climate. These mountain ranges partition the setting into a generally wet region on the upwind flank of the mountains
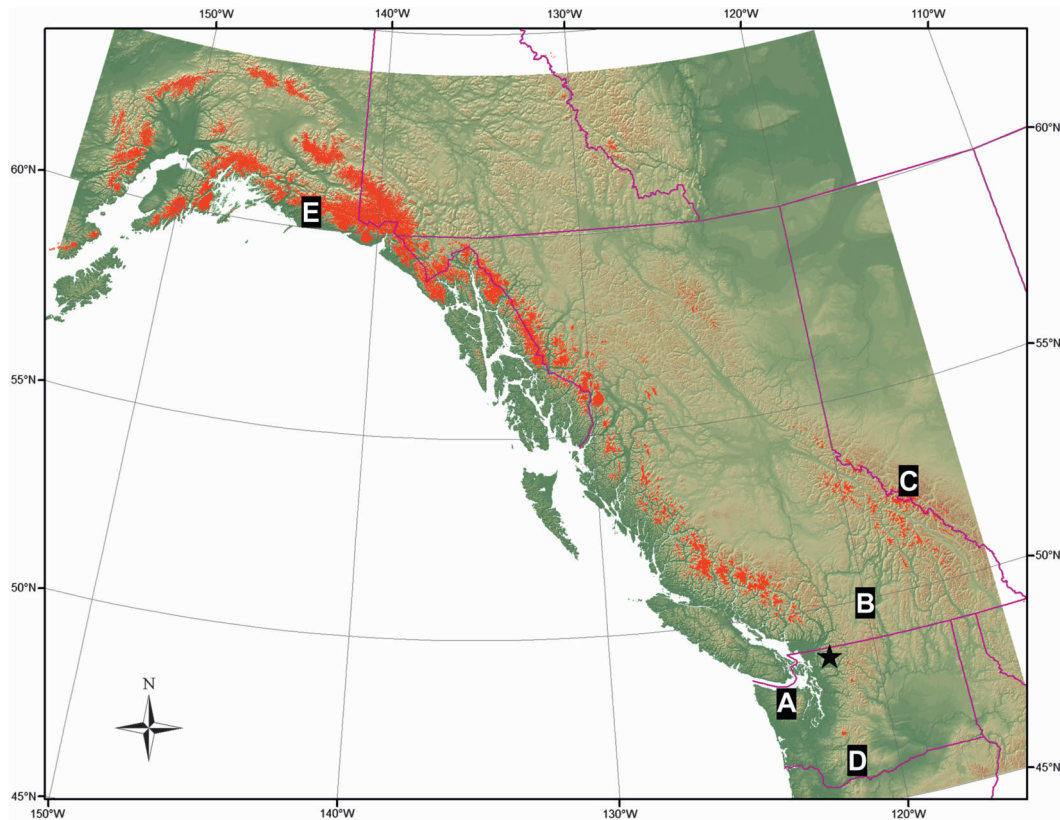
FIG. 1. Glaciers in the Pacific Northwest, shown in red. Data from the Global Land Ice Monitoring from Space (GLIMS) project (http://www.glims.org/). The location of Mount Baker is denoted with a star. Also indicated in the figure are the locations where glacier model sensitivity is tested. Figure courtesy of Harvey Greenberg.

and a dry region toward the leeward interior. On a smaller scale, not resolved in Fig. 2, there are distinct patterns in climate over the peaks and valleys in the mountain ranges, giving rise to rich and intricate local weather patterns (e.g., Minder et al. 2008; Anders et al. 2007). We address the important effect of these small-scale patterns in section 5. For mean melt-season temperature, the pattern is characterized by the north–south gradient, though cooler temperatures at higher elevations can also be seen.

The major feature of the regional atmospheric circulation pattern is the Aleutian low pressure system. The effects of the dominant modes of climate variability influencing the region [e.g., El Niño (e.g., Wallace et al. 1998), the Pacific decadal oscillation (e.g., Mantua et al. 1997), and Pacific–North American pattern (e.g., Wallace and Gutzler 1981)] can all be understood in terms of how they shift the position and intensity of the Aleutian low. These shifts result in a dipolelike pattern, with storms having a tendency to track either north or south, depending on the phase of the mode, and leaving an anomaly of the opposite sign where the storminess is reduced.

The natural year-to-year variation observed in the region's climate system is well characterized by the standard deviations in annual temperature and precipitation from LW50. Figure 2c shows a simple relationship: the interannual variability of precipitation is higher where the mean precipitation is also high. However, for melt-season temperature, the picture is different. Whereas the mean was dominated by the north–south gradient, the variability of melt-season temperature (Fig. 2d) is higher inland, reflecting the continentality of the climate.

b. Glaciers in the Pacific Northwest

The high annual precipitation totals and widespread high-altitude terrain within this area are conducive to the existence of glaciers. The region's glaciers have been extensively mapped, as have their changes over recent geologic history (e.g., Harper 1993; Hodge et al. 1998; O'Neal 2005; Pelto and Hedlund 2001; Post et al. 1971; Porter 1977; Sapaino et al. 1998; Sidjak and Wheate 1999). The glaciers in the region range from the massive tidewater glaciers in southern Alaska to small ice patches in steep terrain. In this study, we focus on the many temperate alpine glaciers in the area because
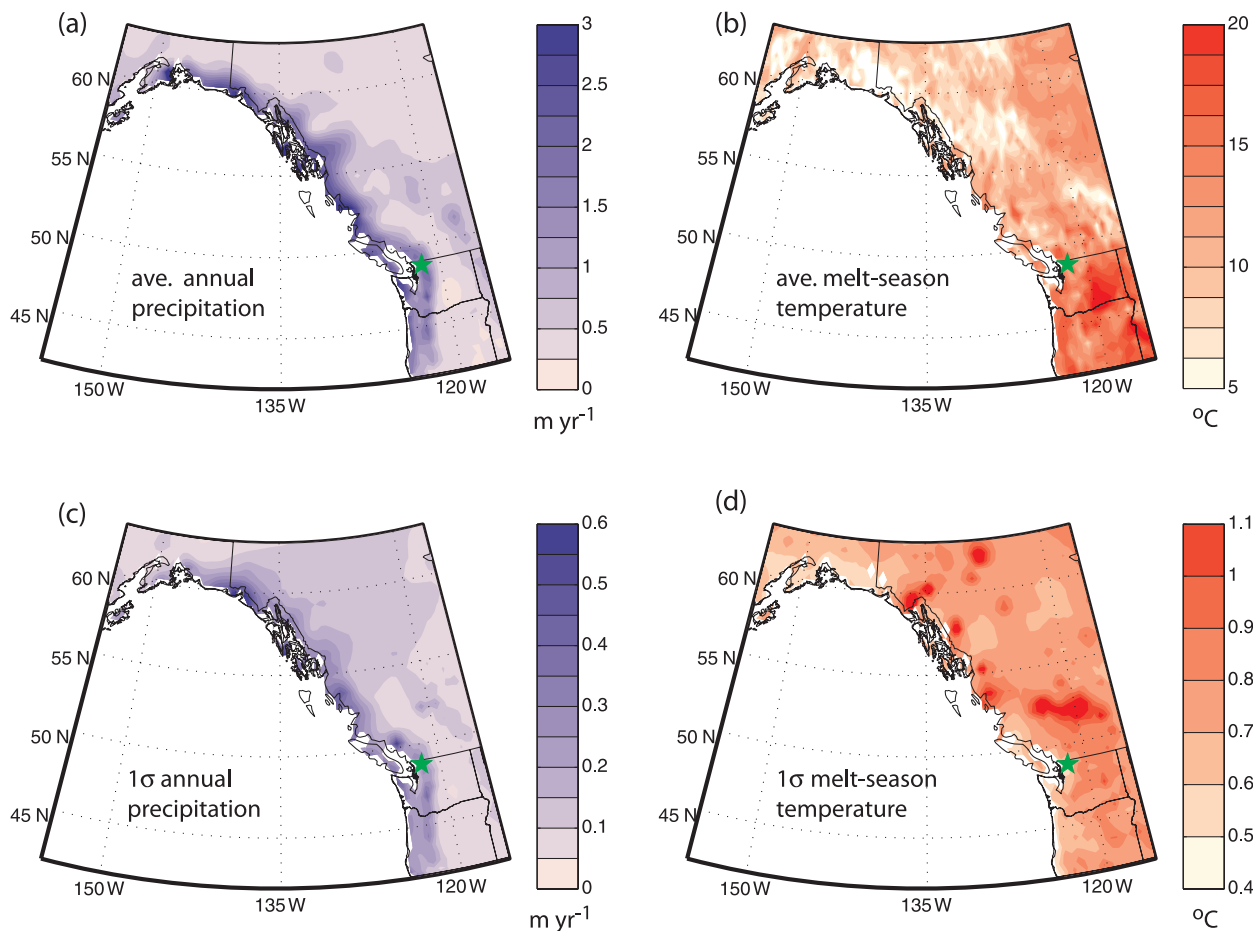
FIG. 2. Climate mean and variability in the Pacific Northwest from LW50: (a) mean annual precipitation (m yr^{-1}), (b) mean melt-season (JJAS) temperature (°C), and interannual standard deviation of (c) mean annual precipitation (m yr^{-1}), and (d) melt-season temperature, in °C.

these are the best suited to reflect a "clean" signature in their response to climate. Even among these temperate glaciers, there is a wide range in size and shape, giving rise to individual variations in advance and retreat.

These advances and retreats cannot be interpreted as responses to long-term climate changes alone. Climate is, by definition, the statistics of weather. In other words, it is the probability density distribution of the full suite of variables that describe the state of the atmosphere over some specified period of interest. (The World Meteorological Organization defines climate as the statistics within any 30-yr period.) A stationary climate, therefore, has constant statistics with a given mean, standard deviation, and higher-order moments. Glaciers are dynamical systems that integrate this natural year-to-year climate variability. This integrative quality of glaciers means that, even in a constant climate, the length of glaciers will vary on decadal and centennial time scales (e.g., Reichert et al. 2002; RO; Roe 2009).

3. A linear glacier model

A schematic of the linear model employed in this study is shown in Fig. 3. The model is from RO, which is based on that of Jóhannesson et al. (1989). The model neglects ice dynamics and assumes that any imbalance between snow accumulation and ice ablation is immediately expressed as a rate of change of the terminus position. Other aspects of the glacier geometry are specified. The absence of glacier flow dynamics means that the linear model is not damped enough on short time scales (e.g., RO), but on decadal time scales and longer this model, and similar ones are able to reproduce realistic glacier variations for realistic climate forcings (Oerlemans 2001; Harrison et al. 2001; RO).

Climate is specified by an annual accumulation rate of P (m yr^{-1}) and an average melt-season temperature T. Ablation is assumed to be linearly proportional to T, where the constant of proportionality is given by the melt-rate factor μ. Observations suggest that μ ranges
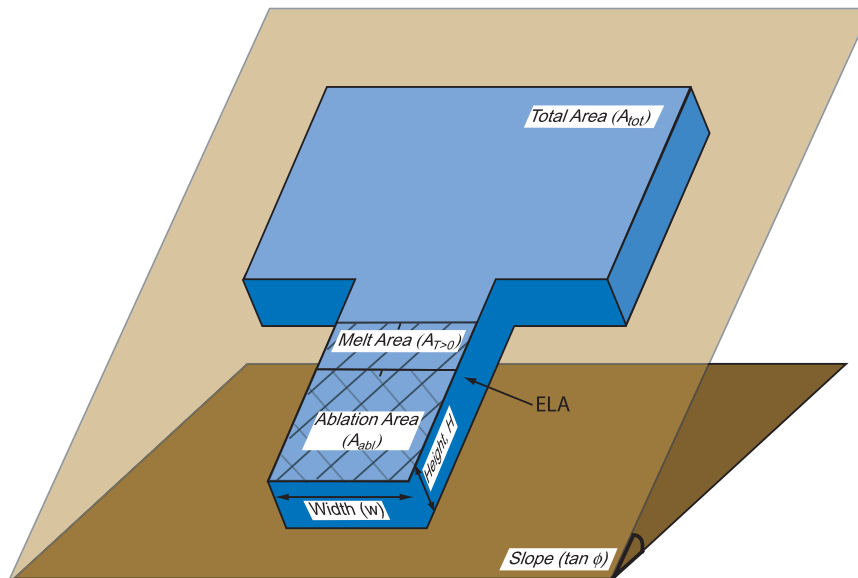
FIG. 3. Schematic of linear glacier model, based on Jóhannesson et al. (1989). Precipitation falls over the entire surface of the glacier (A_{tot}). Melt is linearly proportional to the temperature, and a constant lapse rate is assumed. The basal slope is $\tan\phi$. Melt occurs over the lower reaches of the glacier where melt-season temperature exceeds 0 ($A_{T>0}$), and net mass loss occurs over a smaller area where melting exceeds precipitation (A_{abl}). The upper boundary of this latter region is known as the equilibrium line altitude (ELA). The thickness (H) of the glacier and the width of the ablation area (w) remain constant by assumption.

from 0.50 to 0.84 m yr^{-1} °C^{-1}, water equivalent (e.g., Paterson 1994). The lapse rate Γ is taken to be a constant 6.5°C km^{-1}.

Let $\overline{L}$ be the equilibrium glacier length that would result from constant $\overline{T}$ and $\overline{P}$, the long-term averages of the melt-season temperature and the precipitation. The model calculates the time evolution of perturbation in glacier length L' that arises from the interannual anomalies in the melt-season temperature T' and annual precipitation P'. From here on, we drop the prime symbol and use L, T, and P to represent the anomalies in length, melt-season temperature, and precipitation.

RO show that perturbations in glacier length L away from the equilibrium glacier length for a given constant climate can be described by the following equation:

$$L_{t+\Delta t} = \left(1 - \frac{\mu\Gamma\tan\phi A_{abl}\Delta t}{wH}\right)L_t - \left(\frac{\mu A_{T>0}\Delta t}{wH}\right)T_t$$
$$+ \left(\frac{A_{tot}\Delta t}{wH}\right)P_t \equiv \gamma L_t - \alpha T_t + \beta P_t. \quad (1)$$

The model geometry and parameters are defined in Fig. 3, t is time in years, and Δt is the interval between successive time steps, which we take to be one year. Most of the correlations presented in this paper are calculated with respect to Mount Baker in the Cascade

Mountains of Washington state (48.7°N, 121.8°W). Mount Baker is a large stratovolcano, flanked by eight glaciers with a broad range of sizes and shapes. Mount Baker was chosen because the history of its glaciers is well documented (O'Neal 2005), its climatic setting is well understood, and its glaciers generally fit well into the simple geometrical constraints of the model (i.e., no sharp corners). Doing so also complements the analysis in a companion study (RO).

Table 1 shows the range in the model parameters and geometry that is reasonable for typical Alpine glaciers in this region, taken from RO. Ablation areas are calculated from the total area, using the accumulation area ratio (AAR), the ratio of $1 - A_{abl}$ to A_{tot}, which has been shown to vary from 0.6 to 0.8 in this region (e.g., Porter 1977). For simplicity, we group the parameters for the three terms in (1) into the coefficients γ, α, and β, respectively. Here γ ranges between 0.81 and 0.97 (and is unitless), α between 9 and 81 m °C^{-1}, and β between 85 and 240 yr, depending on the choice of parameters and the size of the glacier. Note that α has the largest uncertainty owing to the large uncertainties in μ and in the AAR, both of which, in principle, can be observed and therefore constrained much better for any specific glacier. Table 1 also shows a standard set of typical parameters, which we use for all calculations from now on, unless otherwise stated.

TABLE 1. Values for geometric parameters that are put into (1) for five glaciers on Mount Baker, Washington (RO). For the values shown here an accumulation area ratio, AAR = 0.7, was assumed. Here A_{tot} is the total glacier area (m^2) and A_{abl} the area over which there is net ablation (m^2); μ is the melt-rate factor (a standard value of 0.67 and a range of 0.5 to 0.84 m yr^{-1} C^{-1} was used), Γ the atmospheric lapse rate (6.5 C km^{-1}), ϕ the slope of the bed, w the average width of the ablation area, H the uniform height (or thickness) of the glacier, and τ is the e-folding relaxation time scale (yr); γ (unitless), α (m °C^{-1}), and β (yr) are combinations of the above variables, as prescribed in (1). In the last column values are generally representative of the Mount Baker glaciers and are used for the standard calculations, unless otherwise noted in the text.

	Boulder	Deming	Coleman	Easton	Rainbow	"Typical"
A_{tot} (km^2)	4.30	5.4	2.1	3.6	2.7	4.0
A_{abl} (km^2)	1.3	1.6	0.64	1.1	0.81	1.2
$\tan\phi$	0.47	0.36	0.47	0.34	0.32	0.4
w (m)	550	450	650	550	300	500
H (m)	50	50	39	51	47	50
τ (yr)	10	9	20	17	13	12
γ	0.90	0.89	0.95	0.94	0.92	0.92
α (m °C^{-1})	32	48	17	26	39	77
β (yr)	160	240	85	130	190	160

Equation (1) describes a glacier that advances (retreats) if melt-season temperatures are anomalously low (high) or if the accumulation is anomalously high (low). It is the discrete form of a simple first-order ordinary differential equation that has a characteristic response time. In the absence of any climate anomalies the glacier asymptotes exponentially back to its equilibrium length with a characteristic e-folding time scale of

$$\tau \equiv \frac{\Delta t}{(1 - \gamma)} = \frac{wH}{\mu \Gamma \tan\phi A_{abl}}.$$

For Mount Baker glaciers, τ ranges from 5 to 30 yr (Table 1), consistent with other estimates for these small mountain glaciers. In the presence of climate forcing, τ represents the decorrelation time scale, or "memory" of the glacier. RO and Roe (2009) demonstrate that, because of this memory, a fundamental property of glaciers is that they will naturally undergo persistent multidecadal and centennial fluctuations, even in the absence of any persistent climate anomalies.

RO also show that this linear model is able to capture typical magnitudes of glacier variations in the Cascade Mountains of Washington State and, so, is adequate to capture the approximate response of glacier length to large-scale patterns of P and T. Caveats and possible improvements to the model are noted in the discussion.

4. Results

a. Glacier correlations

The aim of this study is to explore how patterns of glacier-length variations are driven by patterns of climate. From (1) an expression can be derived for the correlation between the length variations of two glaciers located at two different locations (denoted A and B) in terms of the correlations between T and P:

$$L_{A,(t+1)} = \gamma_A L_{A,t} - \alpha_A T_{A,t} + \beta_A P_{A,t}, \quad (2a)$$

$$L_{B,(t+1)} = \gamma_B L_{B,t} - \alpha_B T_{B,t} + \beta_B P_{B,t}. \quad (2b)$$

The expected value (denoted by angle brackets) of the correlation between glaciers A and B is

$$\langle L_{A,(t+1)} L_{B,(t+1)} \rangle = \gamma_A \gamma_B \langle L_{A,t} L_{B,t} \rangle + \alpha_A \alpha_B \langle T_{A,t} T_{B,t} \rangle$$
$$+ \beta_A \beta_B \langle P_{A,t} P_{B,t} \rangle - \gamma_A \alpha_B \langle L_{A,t} T_{B,t} \rangle$$
$$+ \gamma_A \beta_B \langle L_{A,t} P_{B,t} \rangle - \alpha_A \gamma_B \langle T_{A,t} L_{B,t} \rangle$$
$$+ \beta_A \gamma_B \langle P_{A,t} L_{B,t} \rangle. \quad (3)$$

Cross terms in temperature and precipitation (i.e., $\langle T_{A,t} P_{B,t} \rangle$) have been neglected in (3) because calculations show that in this region they are not statistically significant at a 95% confidence level.

Here $\langle L_{A,t} L_{B,t} \rangle$ is the covariance of L_A and L_B, which is in turn equal to the correlation between L_A and L_B ($\equiv r_{L(A,B)}$), our desired answer, multiplied by the standard deviations of L_A and L_B. The covariances $\langle T_{A,t} T_{B,t} \rangle$ and $\langle P_{A,t} P_{B,t} \rangle$ can be calculated from observations. However, the other terms in (3) are in need of additional manipulation. We elaborate below on $\langle T_{A,t} T_{B,t} \rangle$. The other terms can be derived in a similar fashion.

From the definition of the correlation between T_A and T_B we can write

$$\langle T_{B,t} \rangle = \sigma_{T,B} \left(r_T \frac{\langle T_{A,t} \rangle}{\sigma_{T,A}} + (1 - r_T^2)^{1/2} \nu_t \right), \quad (4)$$

where r_T is the correlation of melt-season temperature between points A and B, $\sigma_{T,()}$ is the standard deviation of T at point (), and we assume that the residual ν_t is a Gaussian-distributed random number of unit variance at time t.

Using the rhs of (4), the value for $\langle L_{A,t} T_{B,t} \rangle$ can be rewritten as

$$\langle L_{A,t} T_{B,t} \rangle = r_T \frac{\sigma_{T,B}}{\sigma_{T,A}} \langle L_{A,t} T_{A,t} \rangle, \qquad (5)$$

where we have used the fact that there is no correlation between a random number and $L_{A,t}$. That is $\langle L_{A,t} \nu_t \rangle = 0$.

So, to find $\langle L_{A,t} T_{B,t} \rangle$ we need $\langle L_{A,t} T_{A,t} \rangle$. First, T_A can be written in terms of its autocorrelation, $\rho_{T,A}$, and the residuals, which we assume are governed by another Gaussian-distributed white noise process, λ_t:

$$T_{A,t} = \rho_{T,A} T_{A,(t-1)} + (1 - \rho_{T,A}^2)^{1/2} \lambda_t. \qquad (6)$$

Therefore, using (6) and (2) we can write

$$\langle L_{A,t} T_{A,t} \rangle = \gamma_A \rho_{T,A} \langle L_{A,(t-1)} T_{A,(t-1)} \rangle - \alpha_A \rho_{T,A} \langle T_{A,(t-1)}^2 \rangle, \qquad (7)$$

where again we use the fact that $\langle L_{A,t} \lambda_t \rangle = 0$.

Since the expected value of a distribution of numbers is independent of the time step $\langle L_{A,t} T_{A,t} \rangle = \langle L_{A,(t-1)} T_{A,(t-1)} \rangle$, we rewrite (7) as

$$\langle L_{A,t} T_{A,t} \rangle = \frac{-\alpha_A \rho_{T,A} \sigma_{T,A}^2}{1 - \gamma_A \rho_{T,A}}. \qquad (8)$$

Therefore, the expected correlation between L_t and T_t is a function of the magnitude of $T(\sigma_T)$, the autocorrelation of $T(\rho_T)$, and the memory of the glacier (γ_A).

Finally, inserting the rhs of (8) into (5) yields

$$\langle L_{A,t} T_{B,t} \rangle = \frac{-\alpha_A r_T \rho_{T,A} \sigma_{T,A} \sigma_{T,B}}{1 - \gamma_A \rho_{T,A}}. \qquad (9)$$

Derivations directly analogous to the above can be used for the remaining terms in (3) and yield an equation for the correlation of glacier lengths between A and B:

$$r_{L(A,B)} = \frac{1}{(1 - \gamma_A \gamma_B) \sigma_{L,A} \sigma_{L,B}} \left[r_T \alpha_A \alpha_B \sigma_{TA} \sigma_{TB} \left(1 + \frac{\gamma_A \rho_{TA}}{1 - \gamma_A \rho_{TA}} + \frac{\gamma_B \rho_{TB}}{1 - \gamma_B \rho_{TB}} \right) \right.$$
$$\left. + r_P \beta_A \beta_B \sigma_{PA} \sigma_{PB} \left(1 + \frac{\gamma_A \rho_{PA}}{1 - \gamma_A \rho_{PA}} + \frac{\gamma_B \rho_{PB}}{1 - \gamma_B \rho_{PB}} \right) \right]. \qquad (10)$$

The terms relating to climate (r_T, r_P, σ_T, σ_P, ρ_T, ρ_P) can all be calculated from observations.

Equation (10) reveals that the correlations between the lengths of glaciers in different places are dependent on both the relationships between climate variables and the geometries of the glaciers in question. The variables and parameters are the correlation of the climate variables (r_T, r_P); the standard deviations of the glacier length (σ_L), precipitation (σ_P), and melt-season temperature (σ_T); the memory of the glacier (γ) and climate (ρ_T, ρ_P); and finally the size and shape of the glacier (α, β). We will now discuss each of these factors in turn and how their respective ranges of uncertainty affect the correlations between glaciers.

b. The spatial correlation of the climate variables

Spatial correlations between glacier behavior are fundamentally driven by spatial correlations in the climate: (10) shows that $r_{L(A,B)}$ is equal to a linear combination of $r_{T(A,B)}$ and $r_{P(A,B)}$. From LW50 we calculate at each grid point the correlations of T and P with their values at Mount Baker (Fig. 4). As expected, r_T and r_P

are high in areas surrounding Mount Baker. However, the spatial extent of significant r_T is much greater than that of r_P. Variations in T are dependent on the perturbations in the summertime radiation balance, which appear to be fairly uniform over the region.

A striking feature of r_P is the antiphasing between Washington and southeastern Alaska. The dipole pattern results from the tendency of storms to be more prevalent in one of the two regions, leaving the other relatively dry. The smaller area of significant values of r_P reflects the smaller spatial scale of precipitation patterns.

c. The relative importance of T and P for a glacier

While the correlations in T and P are the main factors in correlations in L, the relative importance of T or P for glacier length also matters. In what follows, we determine the ratio of length variations forced only by T (denoted as $\sigma_{L,T}$) to length variations forced only by P (denoted as $\sigma_{L,P}$).

These expressions can be derived from (1). Setting $P = 0$, the expected value of a glacier's length forced only by T is
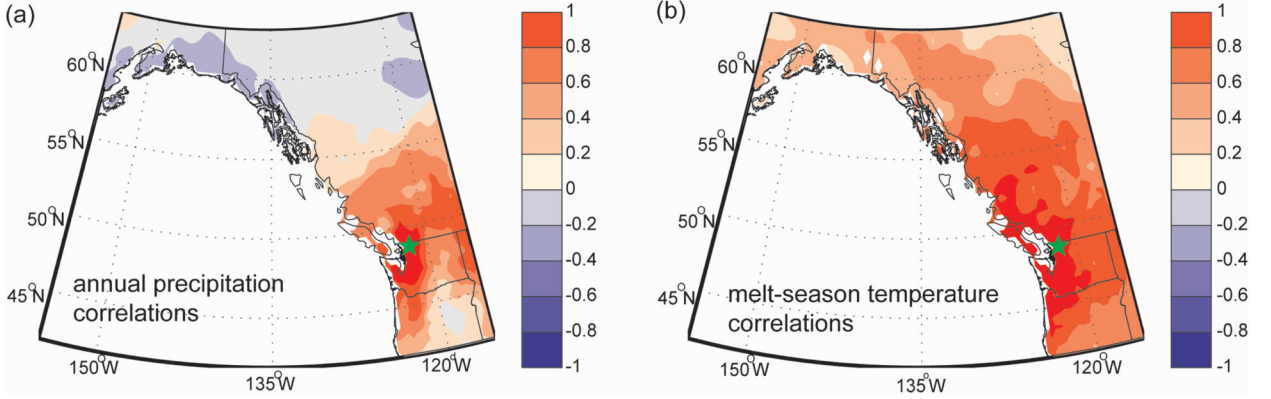
FIG. 4. (a) Correlation in annual mean precipitation between each grid point and Mount Baker, from LW50 dataset; note the dipole of correlations between Alaska and Washington. (b) As in (a), but for the correlation of melt-season temperature; note the widespread correlation of uniform sign over the region. Correlations exceeding about 0.28 would pass a t test at greater than 95% confidence.

$$\langle L_{t+1}^2 \rangle = \gamma^2 \langle L_t^2 \rangle + \alpha^2 \langle T_t^2 \rangle - 2\gamma\alpha \langle L_t T_t \rangle. \quad (11)$$

Using our derivation for $\langle L_t T_t \rangle$ from (8), the variance of the expected length can be written

$$\sigma_L^2 = \gamma^2 \sigma_L^2 + \alpha^2 \sigma_T^2 + \frac{2\gamma\alpha^2 \rho_T \sigma_T^2}{1 - \gamma\rho_T}. \quad (12)$$

Rearranging (12), the standard deviation for a glacier forced only by T is

$$\sigma_{L,T} = \alpha_T \sigma_T \sqrt{\frac{1}{1 - \gamma^2}\left(1 + \frac{2\gamma\rho_T}{1 - \gamma\rho_T}\right)}. \quad (13)$$

Similarly, the expression for a glacier forced only by P is

$$\sigma_{L,P} = \beta_P \sigma_P \sqrt{\frac{1}{1 - \gamma^2}\left(1 + \frac{2\gamma\rho_P}{1 - \gamma\rho_P}\right)}. \quad (14)$$

The ratio R between the two is therefore

$$R = \frac{\sigma_{L,T}}{\sigma_{L,P}} = \frac{\alpha}{\beta}\frac{\sigma_T}{\sigma_P}\sqrt{\frac{1 + [(2\gamma\rho_T)/(1 - \gamma\rho_T)]}{1 + [(2\gamma\rho_P)/(1 - \gamma\rho_P)]}}. \quad (15)$$

From (1), α/β can be rewritten as $\mu A_{T>0}/A_{\text{tot}}$, and the ratio of the glacier length sensitivity to melt-season temperature and precipitation fluctuations can also be written:

$$R = \frac{\sigma_{L,T}}{\sigma_{L,P}} = \frac{A_{T>0}}{A_{\text{tot}}} \cdot \frac{\mu\sigma_T}{\sigma_P} \cdot \sqrt{\frac{1 + [(2\gamma\rho_T)/(1 - \gamma\rho_T)]}{1 + [(2\gamma\rho_P)/(1 - \gamma\rho_P)]}}. \quad (16)$$

The terms $2\gamma\rho_T/(1 - \gamma\rho_T)$ and $2\gamma\rho_P/(1 - \gamma\rho_P)$ in (15) and (16) are similar to one another. Because γ is always less than one and calculations (not given) show that

values for $\rho_{T,P}$ are typically close to 0.2–0.3, the ratio of these terms will be close to one.

To convey a clear sense of the regional coherence of glacier patterns, we present our analyses as if there were a hypothetical glacier at each grid point in the figure. In other words, we imagine that, within each grid point in the LW50, there is a mountain high enough to support glaciers. This is simply a device for clarity of presentation—comparison with real glaciers comes directly from Fig. 1.

Figure 5a shows R for the standard set of parameters. To convey a sense of the uncertainty in R, we also combine the highest melt rate with the lowest AAR and the lowest melt rate with the highest AAR (Figs. 5b and 5c). Overall, the calculations suggest that over most of the area glaciers are more sensitive to melt-season temperature than to precipitation, except for a narrow coastal band where glaciers are always more sensitive to P because of the high precipitation variability and muted melt-season temperature variability (i.e., Fig. 2). However, the extent of T dependence varies greatly depending on the choice of parameters. Glaciers with a high melt factor or a large ablation area are much more likely to be affected by variations in T. In section 5 we explore how small-scale patterns of climate, not resolved at this scale, can affect this answer.

d. Standard deviations

From (10) it can be seen that the standard deviation of T or P and the standard deviation of L affect $r_{L(A,B)}$ directly. Because σ_T and σ_P also strongly influence the sensitivity of glacier length changes (section 4c), their magnitudes can greatly increase or decrease the importance of R and σ_L.

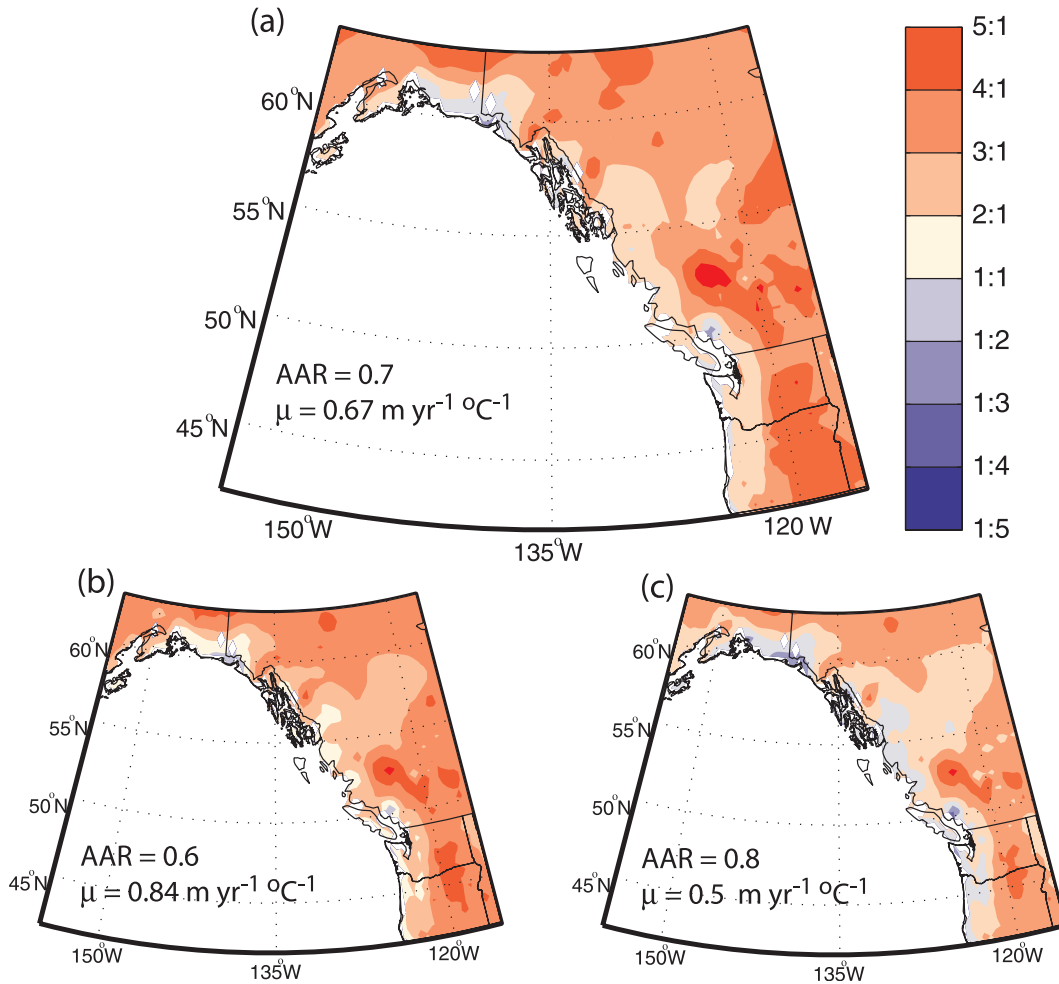We derive a formula for σ_L from the root of the sum of the squares of (13) and (14):

FIG. 5. Ratio of sensitivities to temperature and precipitation for a typical glacier geometry at each grid point for different choice of model parameters. Warm colors denote temperature sensitivity, while cool colors denote sensitivity to precipitation. (a) The standard parameters, (b) the largest ablation area and melt rate factor, and (c) the smallest values of the ablation area and melt rate factor.

$$\sigma_L = \left\{ \frac{1}{1 - \gamma^2} \left[\alpha^2 \sigma_T^2 \left(1 + \frac{2\gamma\rho_T}{1 - \gamma\rho_T} \right) + \beta^2 \sigma_P^2 \left(1 + \frac{2\gamma\rho_P}{1 - \gamma\rho_P} \right) \right] \right\}^{1/2}. \tag{17}$$

Figure 6 shows σ_L for standard parameters; values range from 100 to over 300 m. Along the coasts σ_L is high, and σ_P is also high. Southeast British Columbia also has above-average values in σ_L, corresponding to high values in σ_T.

e. Correlations between glaciers with the same geometry

We now apply (10) to each grid point in LW50 and correlate a hypothetical glacier at that point with a glacier that rests on Mount Baker. We begin by imposing the same γ, α, and β at each point, taking values char-

acteristic for a Mount Baker glacier (Table 1), to eliminate differences in correlation due to geometry and thus isolate the effect of spatial patterns in climate. The effect of differences in geometry and choices in parameters will be addressed in the following section.

Figure 7 shows the expected correlations between a theoretical glacier at each point and a glacier resting on Mount Baker. The correlations between glaciers are strongest where both T and P are well correlated with Mount Baker. On the southeast coast of Alaska r_L is somewhat negative, where P is most strongly anti-correlated with Mount Baker and the glaciers are most
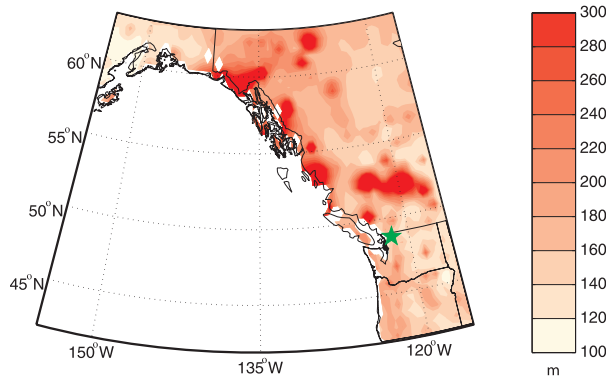
FIG. 6. Standard deviations of glacier length at each grid point if a typical glacier exists at each grid point, calculated from (17). Large standard deviations in length are driven by large standard deviations in either precipitation or temperature (cf. with Fig. 2).

FIG. 7. Correlations between a typical glacier at each grid point and at Mount Baker, calculated from (9).

sensitive to P. These results are consistent with those of Bitz and Battisti (1999). There are also regions where T dominates. For example, the strong sensitivity to T northeast of Mount Baker (Fig. 5), where r_T is also high (Fig. 4b), gives rise to strong glacier correlations. Little to no correlation can be expected in regions where both the T and P correlations with Mount Baker are low and the value of R is ambiguously close to one, such as is the case in northern British Columbia and the Yukon Territory of Canada.

Inferences of the spatial extent of past climate changes are often made by comparing the reconstructed dates of relict moraines. Given the point made in this study that regional correlations in glaciers also arise from natural interannual variability alone (i.e., in a constant climate), there is some chance that concurrent advances would be misinterpreted. Furthermore, the statistical significance of a hypothesized change in climate is difficult to establish from the few points that are typically available from even well-dated moraines. The integrative nature of a glacier gives it a memory of previous climate states and means that the number of independent observations is much lower than the number of years in a record. In the appendix, we show calculations for deriving the appropriate number of degrees of freedom using our model, given the autocorrelation of both the glaciers and the T and P values.

f. Correlations between glaciers with differing geometries

Assuming that all glaciers have the same geometry is clearly a simplification. We expect the spatial correlation between glaciers to weaken if we compare glaciers of different geometries. Because we cannot present the full range of glacier geometries at every point, we focus on locations that are representative of the range of dif-
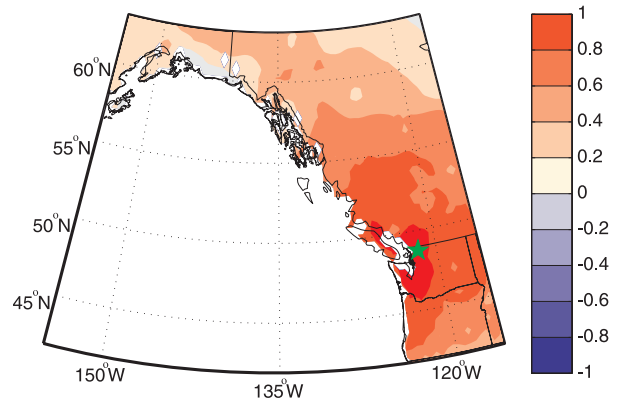
ferent climatic correlations with Mount Baker. These locations, shown in Fig. 1, were chosen to encompass as large a range as possible for this region of r_P, r_T, and R values and are detailed in Table 2.

We consider five combinations of glacier parameters (the five main glaciers of Mount Baker, given in Table 1) and three values for the AAR at each of the five points. Then we correlated the terminal advance and retreat with that of a typical glacier on Mount Baker, with an AAR of 0.7 and μ of 0.67 m yr^{-1} °C^{-1}. The values of r_L calculated with respect to Mount Baker, as well as r_T and r_P, are shown in Fig. 8.

The correlations are strikingly insensitive to this range of parameter variations. Here r_T and r_P are the main drivers of the correlation between glaciers. Differences in the basic geometry are of secondary importance. To the extent that parameters do matter, the variations in the AAR and μ are of most importance (RO).

5. Small-scale patterns

While the LW50 dataset has the advantage of a long record, it lacks the small-scale detail of climate patterns due to individual mountain peaks and valleys that strongly influence the behavior of individual glaciers.

TABLE 2. Key points to correlate with Mount Baker over a variety of glacier geometries: the latitude and longitude of each point are listed, as well as the correlations in precipitation (r_P) and temperature (r_T) and the sensitivity ratio (R). See Fig. 8.

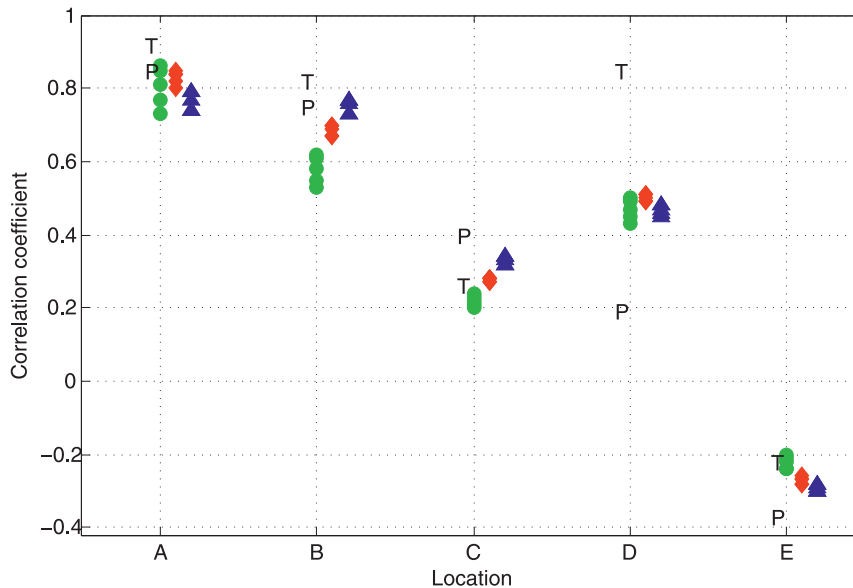| Point	Lat (°N)	Lon (°W)	Nearest mountain	r_P	r_T	R
A	47.3	123.7	Olympus	0.85	0.92	0.39
B	49.8	120.2	Girabaldi	0.75	0.82	2.10
C	53.3	116.8	Columbia Ice Field	0.40	0.26	2.00
D	46.3	119.8	Adams	0.19	0.85	2.40
E	60.3	142.7	Wrangell	−0.37	0.22	0.41

FIG. 8. Sensitivity test of correlations, at selected locations (see Fig. 1), to varying the glacier geometry and parameters: T and P denote melt-season temperature and annual precipitation correlations between that location point and Mount Baker. Colored symbols represent the correlation of glacier length between that location and Mount Baker, and the range arises from using the five different parameter sets applying to the different Mount Baker glaciers (given in Table 1). Finally the different colors mean a different AAR was used: green (AAR = 0.6), red (AAR = 0.7), and blue (AAR = 0.8).

Since 1997 the fifth-generation Pennsylvania State University–National Center for Atmospheric Research Mesoscale Model (MM5) (Grell et al. 1995) has been run (by the Northwest Regional Modeling Consortium at the University of Washington) at 4-km horizontal resolution over the Pacific Northwest (Mass et al. 2003; Anders et al. 2007; Minder et al. 2008). Though the short interval of the model output makes statistical confidence lower, it is instructive to evaluate the patterns of temperature and precipitation over the region on such a fine grid and repeat the calculations that we performed using LW50. RO find good correspondence between the MM5 output and snowpack telemetry (SNOTEL) observations in the vicinity of Mount Baker. The performance of the MM5 model in this region, relative to observations, has also been evaluated by Colle et al. (2000).

The patterns in the mean annual precipitation in Washington State (Fig. 9a) are dominated by the Olympic and Cascade Mountains. Localized maxima in precipitation near individual volcanic peaks can be identified. The pattern of interannual variability of annual precipitation, measured by the standard deviation, is similar to the pattern of the mean precipitation. Mean melt-season temperatures in the region (Fig. 9b) are dominated by elevation differences, with colder temperatures recorded in the mountains. Interannual variability in the mean melt-season temperature, in contrast with precipitation,

is fairly uniform over the region (Fig. 9d), but the amplitude is increased somewhat and exceeds $1°C \ yr^{-1}$ in places (Fig. 9b).

Using (15), the spatial pattern in R can be plotted for the standard set of parameters (Fig. 10). Owing to the high interannual variability in annual precipitation, the variability of glaciers in the Cascades and Olympic Mountains is predicted to be most sensitive to variability in precipitation. This is confined to the high elevations. Lower elevation points, dominated by temperature variability, are not able to sustain actual glaciers in the modern climate.

The high levels of precipitation variability in the mountains also drive high values of the standard deviation in glacier length, exceeding 1400 m in places (Fig. 11). By definition of the standard deviation, the glacier would spend approximately 30% of its time outside of the $\pm 1\sigma$. Thus over the long term, fluctuations of 2–3 km in glacier length should be expected, driven solely by the interannual variability inherent to a constant climate (RO). This result highlights the crucial importance of knowing small-scale patterns of climate in mountainous regions in determining the response of glaciers.

On this spatial scale, interannual climate variations from the MM5 model output are very highly correlated in space. This translates into very high spatial correlations in glacier response (not shown).
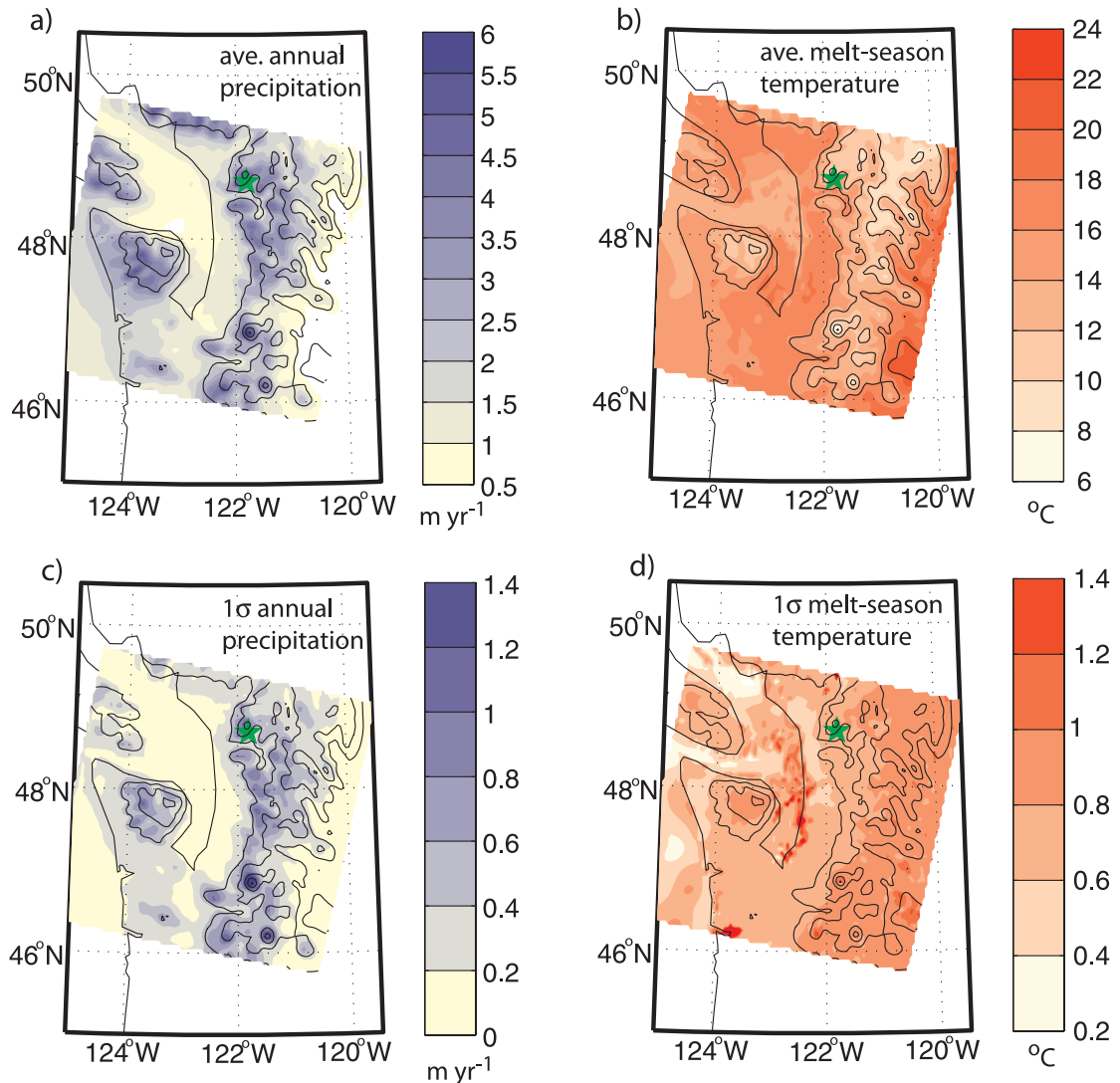
FIG. 9. Archived output from the MM5 numerical weather prediction for the Pacific Northwest at 4-km scale: (a) mean annual precipitation, (b) mean melt-season temperature, and standard deviation of (c) precipitation and (d) melt-season temperature. Contours of the model surface elevation are also plotted every 500 m; the location of Mount Baker is indicated with a star. Note the small-scale patterns of climate associated with the mountainous terrain, in particular the high rates of orographic precipitation.

6. Summary and discussion

A simple linear glacier model has been combined with climate data to address how regional-scale patterns in precipitation and melt-season temperature combine to produce regional-scale patterns in glacier response. In our model framework, correlations in the glacier lengths are a linear combination of the spatial correlations in the climate variability. The climate correlations are modified by the relative importance of temperature and precipitation to the glacier response, which in turn is a function of the glacier geometry and mass balance parameters.

In coastal regions high precipitation variability and low melt-season temperature variability mean that the patterns of glacier response are controlled by the patterns of precipitation variation. Conversely, in continental climates patterns of glacier response are most influenced by the patterns in melt-season temperature. Results are quite insensitive to variations in glacier geometry—it is the spatial patterns in T and P that are the key drivers of spatial patterns in glacier variations.

Finally, using seven years of archived output from a high-resolution numerical weather prediction model shows that the increased total precipitation and precipitation variability characteristic on individual coastal mountain
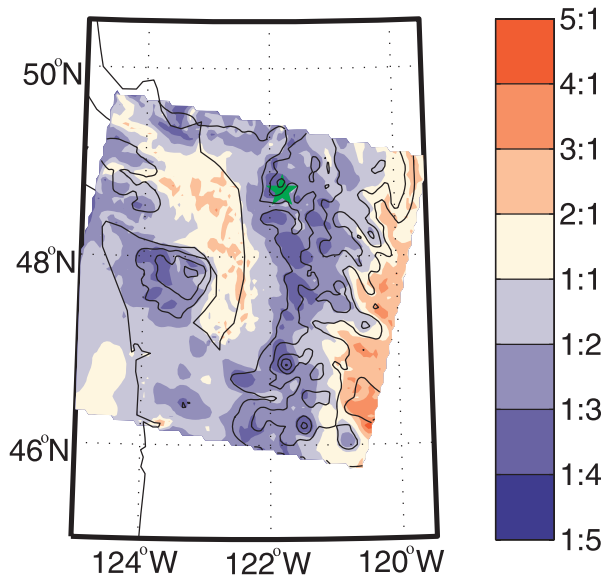
FIG. 10. Ratio of sensitivities to temperature and precipitation of a glacier length with a typical Mount Baker–like geometry, calculated at every model grid point from (16). Blue indicates a greater sensitivity to precipitation. The mountainous regions of the Olympics and Cascades, where glaciers in the region actually exist, are dominated by sensitivity to variation in the precipitation.
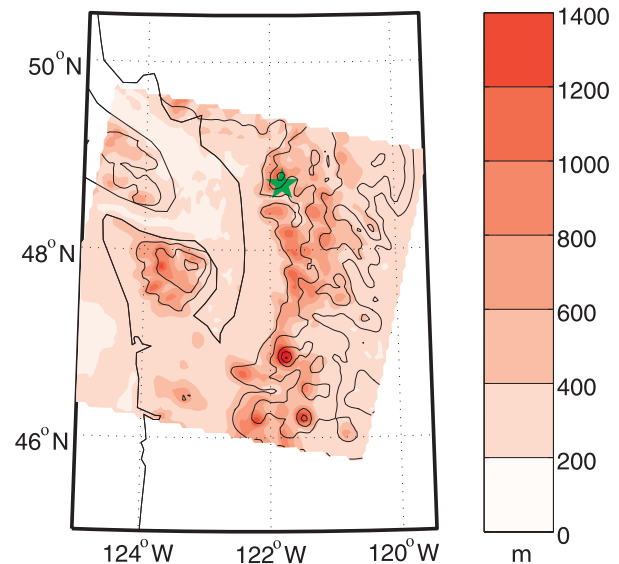
FIG. 11. The standard deviation of glacier length calculated from (17) using the 4-km resolution MM5 output. This fine-resolution scale shows that, in the mountainous regions where glaciers exist, the standard deviation in glacier length is much higher than in lower elevations. The high standard deviations are driven by the high variability in precipitation there.

peaks will give rise to large variations in glacier advance and retreat.

The correlations calculated in this study are derived using a simple model and a grid size larger than the area of a single glacier and, so, should be regarded as providing insight and not predictions. In exchange for being able to understand and analyze the results of the system, we have neglected many of the complications that exist in true dynamical glacier systems and mountain climates. We feel confident that our choice in LW50 is adequate, as the North American Regional Reanalysis model and the 40-yr European Centre for Medium-Range Weather Forecasts (ECMWF) Re-Analysis (ERA-40) grid-spaced dataset produced very similar results. However, climate data with a resolution of 0.5° cannot capture the full gamut of climatic effects in mountainous terrain. The unresolved details of small-scale precipitation patterns will not change the results regarding the overall contrast between maritime and continental climates or the general north–south trends due to the inherent spatial scale of the regional climate patterns. It is likeliest to make a difference in the predicted sensitivities of, and spatial correlations among, the coastal Pacific Northwest glaciers. The lesson from the MM5 results about the importance of knowing small-scale orographic precipitation patterns is one of the key findings of this study.

We also opted to present results in terms of the correlation between glaciers. An alternative would have been to calculate empirical orthogonal functions (EOFs) to find the modes that account for the largest proportion of the variance in glacier advance and retreat. Different treatments for the mass balance are also possible: we could have chosen to use a positive degree-day model (e.g., Braithwaite and Zhang 2000) or a full surface energy balance model (e.g., Rupper 2007) to calculate glacier mass balance. The assumption that all precipitation is accumulation over the glacier could be relaxed by including a temperature-dependent threshold for snow. We feel that this would be unlikely to make any important difference in our main results.

We have also made significant assumptions regarding glacial processes. Chief among these assumptions is the neglect of glacier dynamics. However, several studies have shown that the linear model is capable of reproducing reasonable variations in glacier length (e.g., Jóhannesson et al. 1989; Oerlemans 2005; RO) and, so, is adequate for the purposes of the present study. Glacier geometry is also highly simplified in the linear model. Tangborn et al. (1990) concluded that area distribution of each glacier was the main distinguishing characteristic accounting for difference in mass balance on two adjacent glaciers in the North Cascade Range of Washington State between 1947 and 1961, highlighting the complexities in small-scale geometric and climatic factors relevant to glaciers.

Finally, we have focused on glaciers for which the connection with temperature and precipitation is clear

and well understood. Our framework cannot be directly applied to tropical or tidewater glaciers, glaciers with a history of surging, or large ice caps or ice sheets, where the physics of that connection is more complex. Further work should be performed, understanding not only spatial patterns in glacial correlation but temporal patterns as well. The model can also readily be used to evaluate when and where a climatic trend in glacier length can be detected against the background interannual climatic variability.

APPENDIX

Autocorrelation: Determining the Degrees of Freedom

The autocorrelation of a glacier significantly constrains the number of degrees of freedom (d.o.f) available to qualify the significance of an observed r_L. The greater the time scale, the more a glacier is influenced by its previous states, so fewer statistically independent observations are obtainable in a given interval of time. This glacier memory increases the likelihood that, simply by chance, high correlations will be observed between glaciers. To determine the proper confidence

intervals, the correct number of d.o.f. for a given length of time must be calculated. To do so we must also derive an equation for ρ_L.

The autocorrelation of the length is described by finding the covariance between the lengths from one time step to the next:

$$\langle L_{t+1}L_t \rangle = \gamma^2 \langle L_t L_{t-1} \rangle + \alpha^2 \langle T_t T_{t-1} \rangle + \beta^2 \langle P_t P_{t-1} \rangle$$
$$+ \gamma\alpha \langle L_t T_{t-1} + L_{t-1}T_t \rangle$$
$$+ \gamma\beta \langle L_t P_{t-1} + L_{t-1}P_t \rangle. \tag{A1}$$

Multiplying (1) by T_{t-1} and again neglecting the cross terms between T and P,

$$\langle L_t T_{t-1} \rangle = \gamma \langle L_{t-1}T_{t-1} \rangle + \alpha \langle T_{t-1}^2 \rangle. \tag{A2}$$

Utilizing (8) yet again, to replace $\langle L_{t-1}T_{t-1} \rangle$, the length at any given time is related to T at that point at the previous time step:

$$\langle L_t T_{t-1} \rangle = \frac{\gamma\alpha\rho_T\sigma_T^2}{1 - \gamma\rho_{TA}} + \alpha\sigma_T^2. \tag{A3}$$

Because T at time t can be related to temperature at time $t-1$ via its autocorrelation ρ_T^2 at that point, plus random component (6), we write

$$\langle L_{t-1}T_t \rangle = \frac{\alpha\rho_T^2\sigma_T^2}{1 - \gamma\rho_{TA}}. \tag{A4}$$

Using this same derivation for $\langle L_t P_{t-1} + L_{t-1}P_t \rangle$, we enter (A3) and (A4) into (A2). Our equation describing the autocorrelation of the length of the glacier is written as

$$\rho_L = \frac{1}{\sigma_L^2(1-\gamma^2)}\left[\alpha^2\rho_T\sigma_T^2\left(1 + \frac{\gamma^2}{1-\gamma\rho_T} + \frac{\gamma}{\rho_T} + \frac{\gamma\rho_T}{1-\gamma\rho_T}\right) + \beta^2\rho_P\sigma_P^2\left(1 + \frac{\gamma^2}{1-\gamma\rho_P} + \frac{\gamma}{\rho_P} + \frac{\gamma\rho_P}{1-\gamma\rho_P}\right)\right]. \tag{A5}$$

If the autocorrelations in the climate $\rho_{T,P}$ are zero, (A5) will simplify dramatically.

This autocorrelation allows us to determine the input into the Bretherton et al. (1999) formula for determining the correct number of d.o.f. in a time series, given some level of autocorrelation. The autocorrelation of the glacial system requires a much longer record in order to determine a significant correlation than its forcings, which have a much shorter memory.

Therefore, we increase the numbers of d.o.f. by assuming that the 1950–90 detrended values for temperature and precipitation are representative of the range of variation over longer periods of time. This is a reasonable

assumption as the brevity of the detrended T and P data yields a conservative estimate of the climate variations.

REFERENCES

Anders, A. M., G. H. Roe, D. R. Durran, and J. R. Minder, 2007: Small-scale spatial gradients in climatological precipitation on the Olympic Peninsula. *J. Hydrometeor.,* **8,** 1068–1081.

Bitz, C. M., and D. S. Battisti, 1999: Interannual to decadal variability in climate and the glacier mass balance in Washington, western Canada, and Alaska. *J. Climate,* **12,** 3181–3196.

Braithwaite, R. J., and Y. Zhang, 2000: Sensitivity of mass balance of five Swiss glaciers to temperature changes assessed by tuning a degree-day model. *J. Glaciol.,* **46,** 7–14.

Bretherton, C. S., M. Widmann, V. P. Dymnikov, J. M. Wallace, and I. Bladé, 1999: The effective number of spatial degrees of freedom of a time-varying field. *J. Climate,* **12,** 1990–2009.

Chinn, T., S. Winkler, M. J. Salinger, and N. Haakensen, 2005: Recent glacier advances in Norway and New Zealand: A comparison of their glaciological and meteorological causes. *Geogr. Ann.,* **87,** 141–157.

Colle, B. A., C. F. Mass, and K. J. Westrick, 2000: MM5 precipitation verification over the Pacific Northwest during the 1997–99 cool seasons. *Wea. Forecasting,* **15,** 730–744.

Grell, G., J. Dudhia, and D. Stauffer, 1995: A description of the Fifth-Generation Penn State/NCAR Mesoscale Model (MM5). NCAR Tech. Note. NCAR/TN-398+STR, 117 pp.

Hamlet, A. F., P. W. Mote, M. P. Clark, and D. P. Lettenmaier, 2005: Effects of precipitation and temperature variability on snowpack trends in the western United States. *J. Climate,* **18,** 4545–4561.

Harper, J. T., 1993: Glacier terminus fluctuations on Mount Baker, Washington, U.S.A., 1940-1990, and climatic variations. *Arct. Alp. Res.,* **25,** 332–340.

Harrison, W. D., D. H. Elsberg, K. A. Echelmeyer, and R. M. Krimmel, 2001: On the characterization of glacier response by a single time-scale. *J. Glaciol.,* **47,** 659–664.

Hodge, S. M., D. C. Trabant, R. M. Krimmel, T. A. Heinrichs, R. S. March, and E. G. Josberger, 1998: Climate variations and changes in mass of three glaciers in western North America. *J. Climate,* **11,** 2161–2179.

Jóhannesson, T., C. Raymond, and E. D. Waddington, 1989: Timescale for adjustment of glaciers to changes in mass balance. *J. Glaciol.,* **21,** 355–369.

Legates, D. R., and C. J. Willmott, 1990a: Mean seasonal and spatial variability in gauge-corrected, global precipitation. *Int. J. Climatol.,* **10,** 111–127.

——, and ——, 1990b: Mean seasonal and spatial variability in global surface air temperature. *Theor. Appl. Climatol.,* **41,** 11–21.

Mantua, N. A., S. R. Hare, Y. Zhang, J. M. Wallace, and R. C. Francis, 1997: A Pacific interdecadal climate oscillation with impacts on salmon production. *Bull. Amer. Meteor. Soc.,* **78,** 1069–1079.

Mass, C. F., and Coauthors, 2003: Regional environmental prediction over the Pacific Northwest. *Bull. Amer. Meteor. Soc.,* **84,** 1353–1366.

Minder, J. M., D. R. Durran, G. H. Roe, and A. M. Anders, 2008: The climatology of small-scale orographic precipitation over the Olympic Mountains: Patterns and processes. *Quart. J. Roy. Meteor. Soc.,* **134,** 817–839.

Mölg, T., and D. R. Hardy, 2004: Ablation and associated energy balance of a horizontal glacier surface on Kilimanjaro. *J. Geophys. Res.,* **109,** D16104, doi:10.1029/2003JD004338.

Nesje, A., 2005: Briksdalsbreen in western Norway: AD 1900-2004 frontal fluctuations as a combined effect of variations in winter precipitation and summer temperature. *Holocene,* **15,** 1245–1252.

Oerlemans, J., 2001: *Glaciers and Climate Change.* AA Balkema Publishers, 160 pp.

——, 2005: Extracting a climate signal from 169 glacier records. *Science,* **308,** 675–677.

Ohmura, A., P. Kasser, and M. Funk, 1992: Climate at the equilibrium line of glaciers. *J. Glaciol.,* **38,** 397–411.

——, M. Wild, and L. Bengtsson, 1996: A possible change in mass balance of Greenland and Antarctic ice sheets in the coming century. *J. Climate,* **9,** 2124–2135.

O'Neal, M. A., 2005: Late Little Ice Age glacier fluctuations in the Cascade Range of Washington and northern Oregon. Ph.D. dissertation, Dept. of Earth and Space Science, University of Washington, 117 pp.

Paterson, W. S. B., 1994: *The Physics of Glaciers.* 3rd ed. Pergamon Press, 480 pp.

Pelto, M. S., and C. Hedlund, 2001: Terminus behavior and response time of North Cascade glaciers, Washington, U. S. A. *J. Glaciol.,* **47,** 497–506.

Porter, S., 1977: Present and past glaciation threshold in the Cascade Range, Washington, USA: Topographic and climatic controls and paleoclimatic implications. *J. Glaciol.,* **18,** 101–116.

Post, A., D. Richardson, W. V. Tangborn, and F. L. Rosselot, 1971: Inventory of glaciers in the North Cascades, Washington. USGS Professional Paper 705-A, 26 pp.

Putkonen, J., and M. O'Neal, 2006: Degradation of unconsolidated Quaternary landforms in the western North America. *Geomorphology,* **75,** 408–419.

Reichert, B. K., L. Bengtsson, and J. Oerlemans, 2002: Recent glacier retreat exceeds internal variability. *J. Climate,* **15,** 3069–3081.

Roe, G. H., 2009: Feedbacks, time scales, and seeing red. *Annu. Rev. Earth Planet. Sci.,* **37,** 93–115, doi:10.1146/annurev. earth.061008.134734.

——, and M. A. O'Neal, 2009: The response of glaciers to intrinsic climate variability: Observations and models of late Holocene variations. *J. Glaciol.,* in press.

Rupper, S. B., 2007: Glacier sensitivity and regional climate: Past and present. Ph.D. dissertation, Dept. of Earth and Space Sciences, University of Washington, 276 pp.

——, and G. H. Roe, 2008: Glacier changes and regional climate: A mass and energy balance approach. *J. Climate,* **21,** 5384–5401.

Sapaino, J. J., W. D. Harrison, and K. A. Echelmeyer, 1998: Elevation, volume and terminus changes of nine glaciers in North America. *J. Glaciol.,* **44,** 119–135.

Sidjak, R. W., and R. D. Wheate, 1999: Glacier mapping of the Illecillewaet icefield, British Columbia, Canada, using Landsat TM and digital elevation data. *Int. J. Remote Sens.,* **20,** 273–284.

Tangborn, W. V., A. G. Fountain, and W. G. Sikonia, 1990: Effect of area distribution with altitude on glacier mass balance—A comparison of North and South Klawatti glaciers, Washington State, U.S.A. *Ann. Glaciol.,* **14,** 278–282.

Wallace, J. M., and D. S. Gutzler, 1981: Teleconnections in the geopotential height field during the Northern Hemisphere winter. *Mon. Wea. Rev.,* **109,** 784–812.

——, E. M. Rasmusson, T. P. Mitchell, V. E. Kousky, E. S. Sarachik, and H. von Storch, 1998: On the structure and evolution of ENSO-related climate variability in the tropical Pacific: Lessons from TOGA. *J. Geophys. Res.,* **103,** 14 241–14 259.